ENGINEERING RESEARCH INSTITUTE
UNIVERSITY OF MICHIGAN
ANN ARBOR

TECHNICAL REPORT NO. 5

EXPERIMENTS CONCERNING THE YIELD SURFACE AND THE ASSUMPTION OF LINEARITY IN THE PLASTIC STRESS-STRAIN RELATIONS

BY

P. M. NAGHDI
J. C. ROWLEY
C. W. BEADLE

Project 2027

OFFICE OF ORDNANCE RESEARCH, U.S. ARMY
CONTRACT NO. DA-20-018-ORD-12099
PROJECT NO. TB-20001(234), DA PROJECT 599-01-004

April, 1954

ABSTRACT

Combined tension and torsion experiments for 14 tabular 24S-T4 aluminum alloy specimens with considerable initial anisotrophy are reported. In all cases, the results reveal the existence of corners on the yield loci of the material.

EXPERIMENTS CONCERNING THE YIELD SURFACE AND THE ASSUMPTION OF LINEARITY IN THE PLASTIC STRESS-STRAIN RELATIONS

INTRODUCTION—GENERAL BACKGROUND

In a recent paper (1)[1] experimental results on combined tension and torsion of tubular specimens made of aluminum alloy which possessed an appreciable initial anisotrophy were reported. In these tests the variable loading path was such that tension was followed by torsion and permitted the determination of the initial shear modulus G_i when twist began. The modulus G_i, for all ratios of the increment of axial stress to the increment of shearing stress ($d\sigma_{33}/d\sigma_{23}$) during loading, was found to be considerably less than the elastic shear modulus G_o, except when unloading had actually taken place; furthermore, it was repeatedly observed that plastic strains were produced for some negative values of $d\sigma_{33}/d\sigma_{23}$ ($d\sigma_{zz}/d\tau_{\theta z}$).

These results motivated further experimental investigation on the character of the yield loci and the possible validity of the assumption of linearity of the increment of the plastic strains in the increment of the stresses (hereafter referred to as the assumption of linearity). We recall that in the expression for the increment of the plastic strain tensor $d\vec{\epsilon}''_{ij}$ in terms of a plastic potential f, namely,

$$d\epsilon''_{ij} = H \frac{\partial f}{\partial \sigma_{ij}} \, df,$$

the existence of a smooth loading surface (which has a continuous turning tangent) is implied, and furthermore, it is usually assumed that $d\epsilon''_{ij}$ is linear in $d\sigma_{ij}$.

---

[1]Numbers in parentheses refer to the bibliography at the end of the paper.

Let us consider an initially smooth yield locus f_1 as shown in Fig. 1. Since the plastic strain increment vector is normal to the loading surface (2), then if the additional stress increments to produce f_2 and subse-

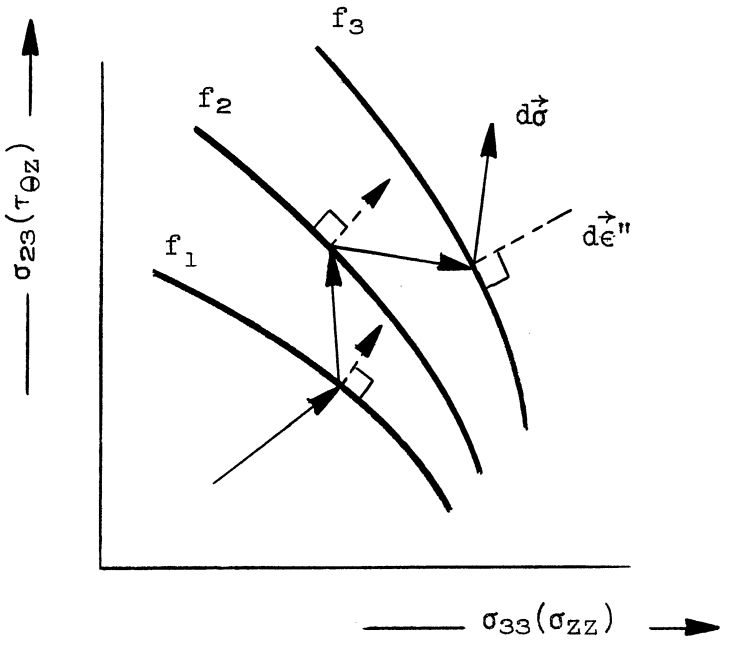

Fig. 1: Relation of stress and plastic strain increment vectors to subsequent smooth yield loci.

quently f_3 are small, the plastic strain increments should be a smooth function of any of the monotonically increasing variables along the stress path. Thus, even if the subsequent loading surfaces were to distort appreciably, the existence of a smooth surface would predict that the increment of the plastic strain vector $d\vec{\epsilon}''$ would at most rotate independent of the wide excursions of the direction of the increment of the stress vector $d\vec{\sigma}$. As pointed out by Drucker and Stokton (2,4), it may be emphasized that this is independent of the assumption of linearity.

If, on the other hand, in producing the subsequent surfaces f_2 and f_3, the direction of $d\vec{\epsilon}''$, depends on the direction of $d\vec{\sigma}$, then the existence of a corner or vertex on the loading surface is possible. Alternatively, since at a corner a unique normal vector is not defined, the direction of the plastic strain increment vector is restricted only to the directions included between the normals to the surface at adjacent points (Fig. 2); thus, the dependence of $d\vec{\epsilon}''$ on $d\vec{\sigma}$ is possible.

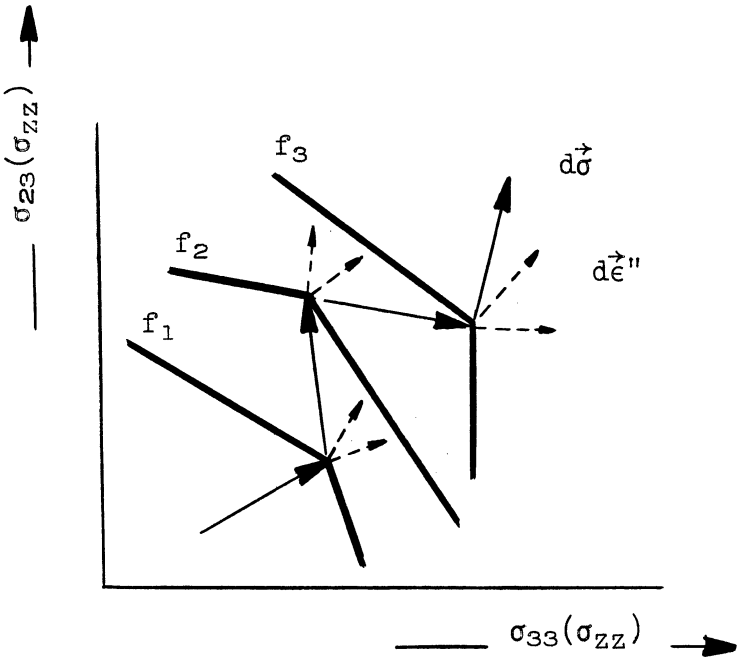

Fig. 2: Relation of stress and plastic strain increment vectors to subsequent yield loci exhibiting corners.

This paper contains experimental results on the evidence of the existence of corners on the yield loci and the possible invalidity of the assumption of linearity of the increment of the plastic strains in the increment of the stresses for an aluminum alloy (24S-T4) which possessed considerable initial anisotropy. The experiments were performed on 14 tubular specimens, some of which were previously subjected to combined tension and torsion (1). In all cases, the loading program in combined tension and torsion was such that small additional "increments" of stress were applied to an already existing plastic state.

SPECIMENS AND EQUIPMENT

The thin-walled specimens were made of 24S-T4 aluminum alloy which possessed considerable initial anisotropy[2]. All specimens used had the nominal

[2]See Fig. 12 of reference 1.

dimensions of 0.75 inch inside diameter and 0.075 inch thickness, some of which had been previously work-hardened. To indicate the history of each specimen prior to the present investigation, it might be helpful to mention that the tubular specimens numbered 50, 52, 57, and 59 (Figs. 4, 5, 6, 7, and 8) were employed in the previous experiment (1); all other specimens, however, were virgin.

The testing machine, the extensometer, the recording instruments, and the associated equipment used in this experiment, together with the accuracies of the resulting measurements, have been described in detail elsewhere (1) and will not be repeated here.

EXPERIMENTAL RESULTS

The experiments conducted were such that the specimens were subjected to an initial tension and torsion (well into the plastic range) followed by increments of tension and torsion. The approximate character of these stress paths are shown in Fig. 3. The test results for the 14 tubular

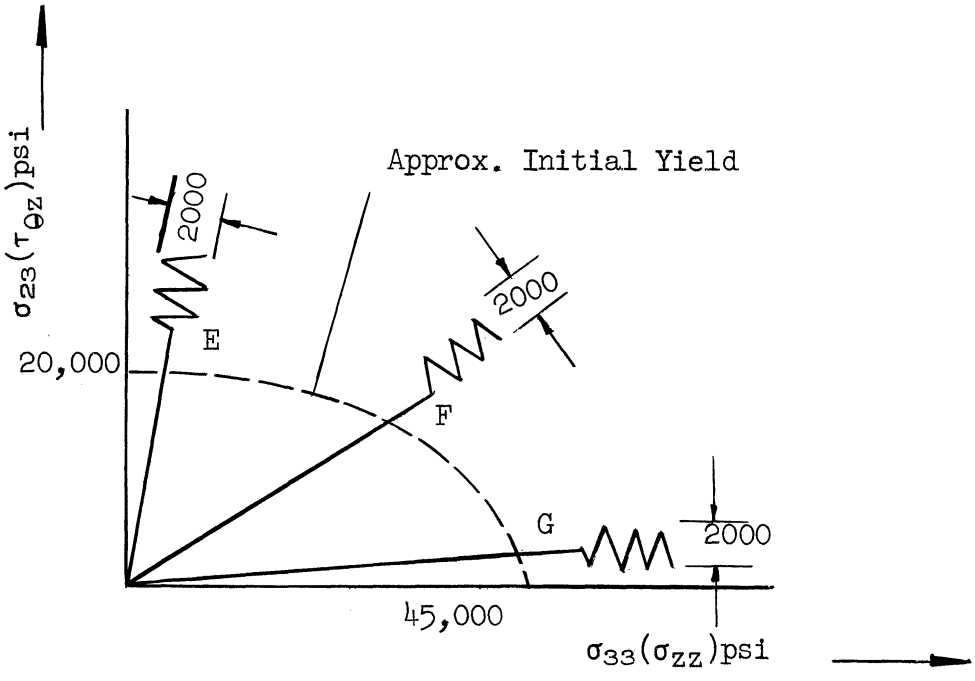

Fig. 3

specimens are shown in Figs. 4 to 17. The test data have been arranged into three groups designated by E, F, and G, according to the region of the stress space, as indicated in Fig. 3. The data for each specimen are presented by three curves which show the variations of the axial and shearing stress, as well as one of the plastic strains, all plotted vs. the other plastic strain (monotonically increasing for that test). The approximate strain rates for each test are also indicated in Figs. 4 to 17. To emphasize the clarity and convenience of the experimental measurements afforded by the continuous recording of all variables, a facsimile of one of the oscillograph films is reproduced in Fig. 18.

Some of the important features of the experimental results with reference to Fig. 4 to 17 will now be discussed. First, note that for all specimens $\epsilon''_{\theta z}$ appears to be uniformly increasing with time, even for small decreasing increments of the shearing stress $\tau_{\theta z}$. This can be seen from Fig. 19, which is a magnified portion of the data of the specimen F-3 (Fig. 11). Furthermore, it is clearly seen that there is a strong correlation between the direction of both stress and strain increment vectors for all three groups of specimens. Specifically, consider the details of this correlation for group E specimens (Figs. 4 to 8). The characters of both ϵ''_{zz} and σ_{zz} versus $\epsilon''_{\theta z}$ curves are oscillatory in nature and appear to be essentially alike. A close examination of these curves seems to indicate: (a) the directions of $d\vec{\epsilon}''$ and $d\vec{\sigma}$ have nearly the same sense along the entire loading path and (b) the magnitude of the strain increment vector is approximately proportional to the magnitude of the stress increment vector, i.e., $|d\vec{\epsilon}''| = m|d\vec{\sigma}|$. In addition, note that, since the proportionality factor m for the initial increment of the stress vector is less than that for subsequent increments of stress (where it seems to remain nearly constant), the occurrence of negative plastic strains beyond the first increment is possible and, in fact, does occur. In a similar manner, corresponding observations may also be made for groups F and G specimens (Figs. 9 to 13 and Figs. 14 to 17). For group F, however, the variation of ϵ''_{zz} versus $\epsilon''_{\theta z}$ curves, although oscillatory, has a definite upward trend.

CONCLUSION

From the experimental results, it is quite clear that for the material tested the yield loci are not smooth. Furthermore, definite evidence of the existence of the corners on the yield loci has been established. In view of this observed character of the yield loci, the validity of the assumption of linearity cannot be ascertained from the present or similar experimental results. It might be, however, that the assumption of linearity, together with the use of a singular yield condition, would correlate these results.

Finally, it should be mentioned that the existence of corners on the yield loci of the material tested confirms and explains previous experimental results (1).

BIBLIOGRAPHY

1. "An Experimental Study of Biaxial Stress-Strain Relations in Plasticity", by P. M. Naghdi and J. C. Rowley, Tech. Rept. No. 2, Engineering Research Institute Project 2027, University of Michigan.

2. "A More Fundamental Approach to Plastic Stress-Strain Relations", by D. C. Drucker, Proc. First U. S. National Congress Appl. Mech. 487-491 (1951).

3. "Instrumentation and Fundamental Experiments in Plasticity", by D. C. Drucker and F. D. Stokton, to appear in the Proc. Soc. Exp. Stress Analysis; also ONR Tech. Rept. No. 68, Brown University, 1952.

4. "Experimental Evidence of Non-Linearity in Plastic Stress-Strain Relations", by F. D. Stokton, ONR Tech. Rept. No. 88, Brown University, 1953.

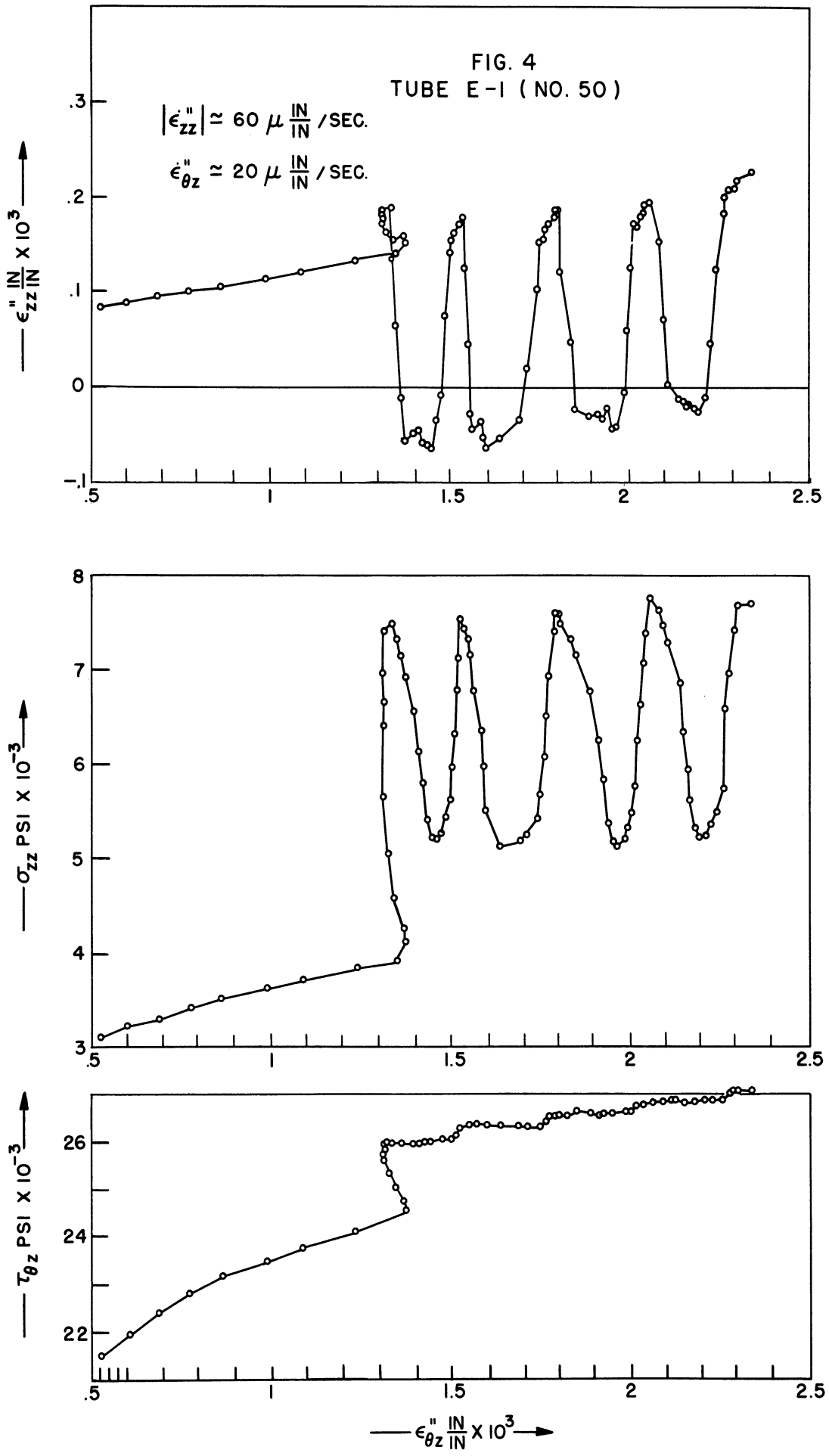
FIG. 4
TUBE E-1 (NO. 50)
$|\dot{\epsilon}''_{zz}| \simeq 60\,\mu\,\frac{IN}{IN}$ / SEC.
$\dot{\epsilon}''_{\theta z} \simeq 20\,\mu\,\frac{IN}{IN}$ / SEC.
$\epsilon''_{zz}\frac{IN}{IN} \times 10^3$
σ_{zz} PSI $\times 10^{-3}$
$\tau_{\theta z}$ PSI $\times 10^{-3}$
$\epsilon''_{\theta z}\frac{IN}{IN} \times 10^3$

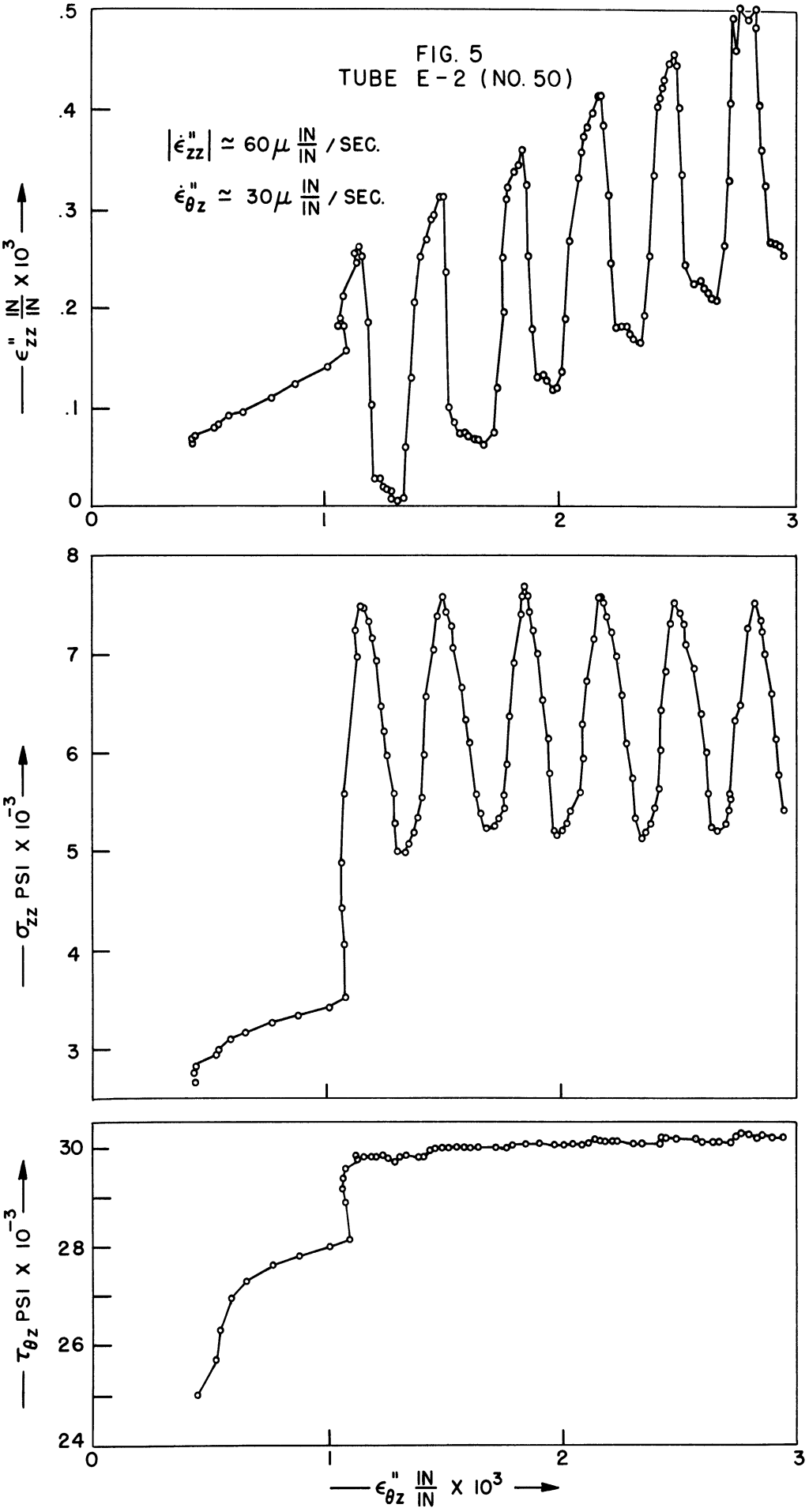
FIG. 5
TUBE E-2 (NO. 50)
$|\dot{\epsilon}''_{zz}| \simeq 60\mu \frac{IN}{IN}$ / SEC.
$\dot{\epsilon}''_{\theta z} \simeq 30\mu \frac{IN}{IN}$ / SEC.
$\epsilon''_{zz} \frac{IN}{IN} \times 10^{3}$
σ_{zz} PSI $\times 10^{-3}$
$\tau_{\theta z}$ PSI $\times 10^{-3}$
$\epsilon''_{\theta z} \frac{IN}{IN} \times 10^{3}$

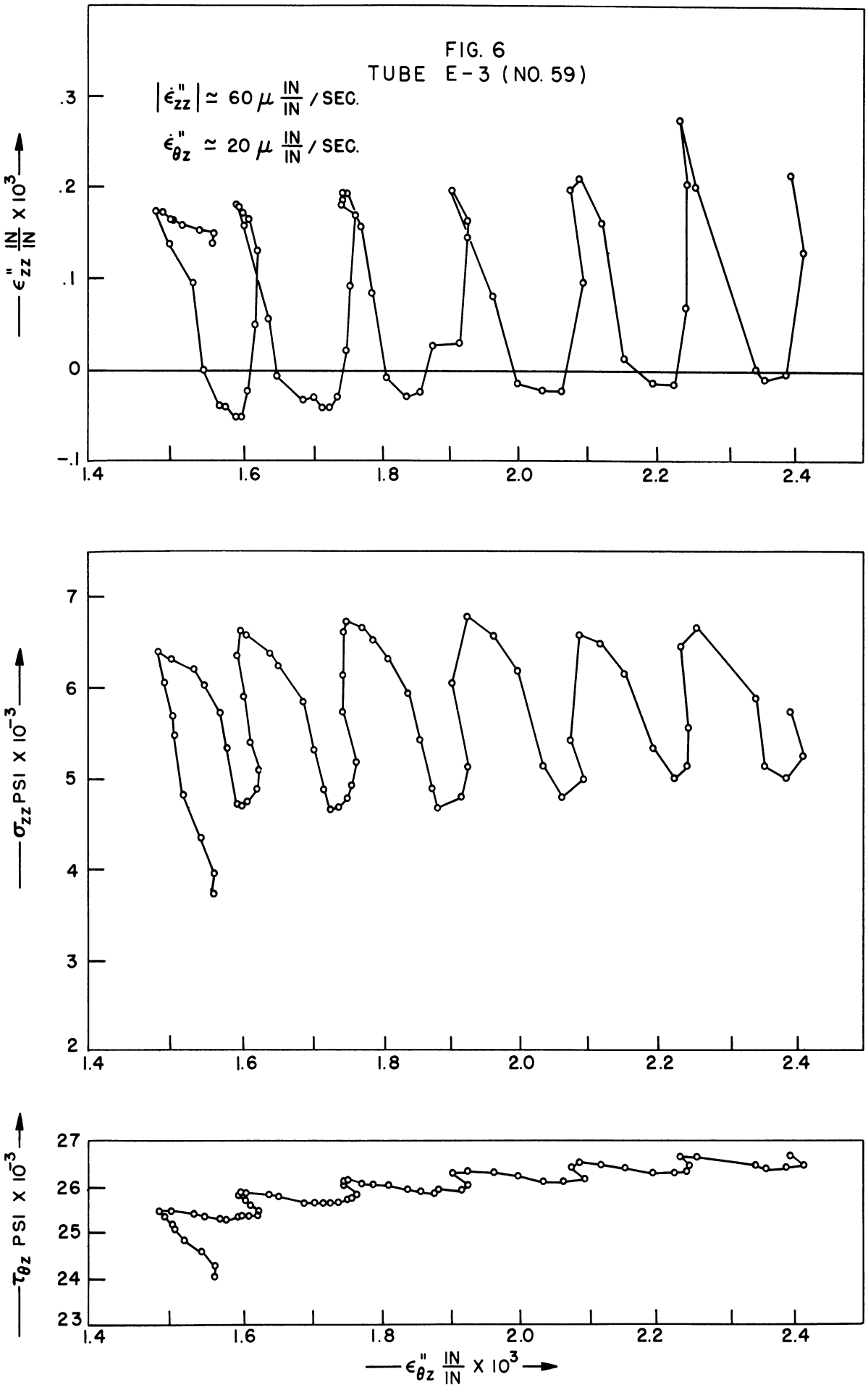
FIG. 6
TUBE E-3 (NO. 59)
$|\dot{\epsilon}''_{zz}| \simeq 60\,\mu\,\frac{IN}{IN}$ / SEC.
$\dot{\epsilon}''_{\theta z} \simeq 20\,\mu\,\frac{IN}{IN}$ / SEC.
$\epsilon''_{zz}\,\frac{IN}{IN} \times 10^3$
σ_{zz} PSI $\times 10^{-3}$
$\tau_{\theta z}$ PSI $\times 10^{-3}$
$\epsilon''_{\theta z}\,\frac{IN}{IN} \times 10^3$

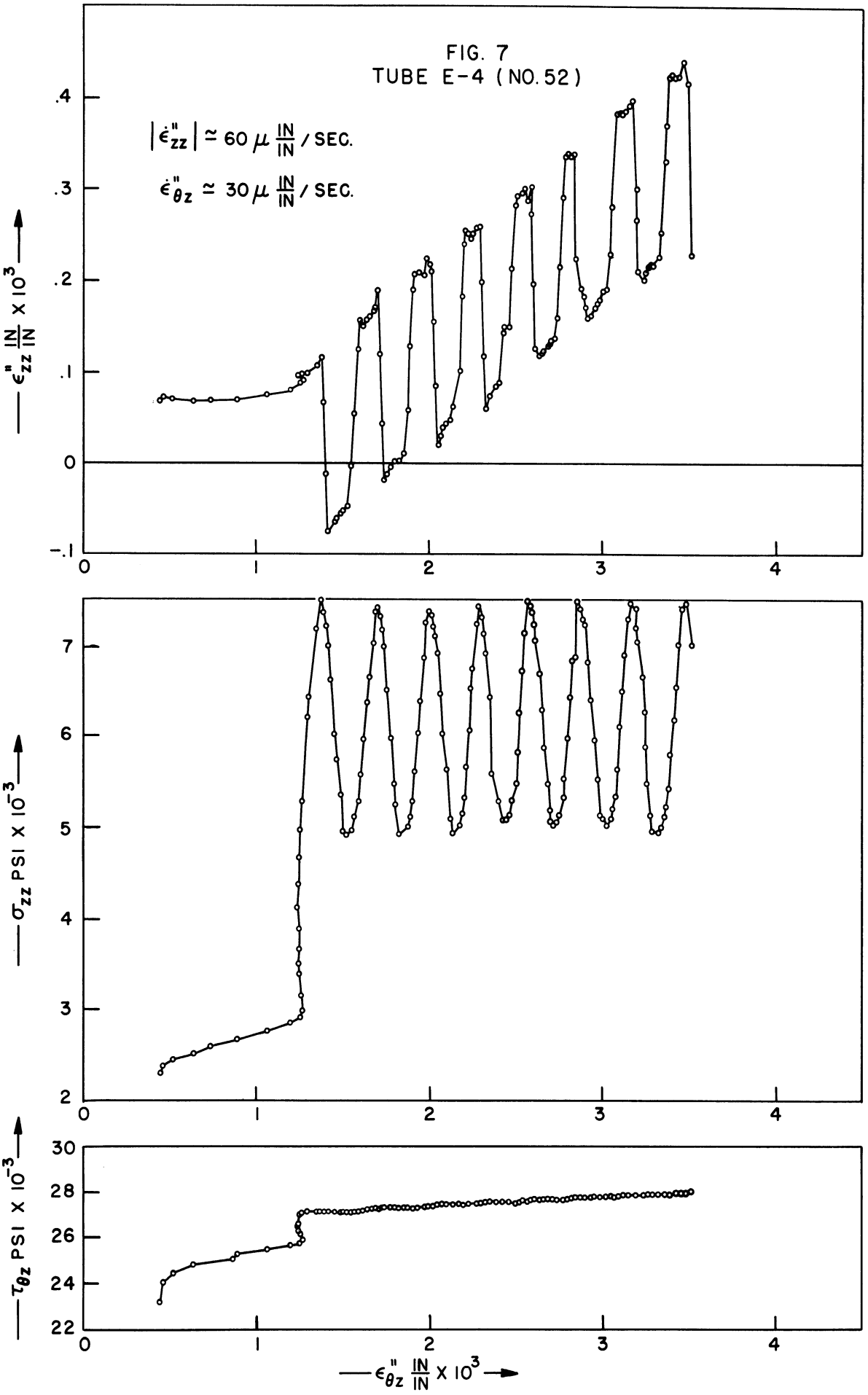
FIG. 7
TUBE E-4 (NO. 52)
$|\dot{\epsilon}''_{zz}| \simeq 60\,\mu\,\frac{IN}{IN}$ / SEC.
$\dot{\epsilon}''_{\theta z} \simeq 30\,\mu\,\frac{IN}{IN}$ / SEC.
$\epsilon''_{zz}\,\frac{IN}{IN} \times 10^3$
σ_{zz} PSI $\times 10^{-3}$
$\tau_{\theta z}$ PSI $\times 10^{-3}$
$\epsilon''_{\theta z}\,\frac{IN}{IN} \times 10^3$

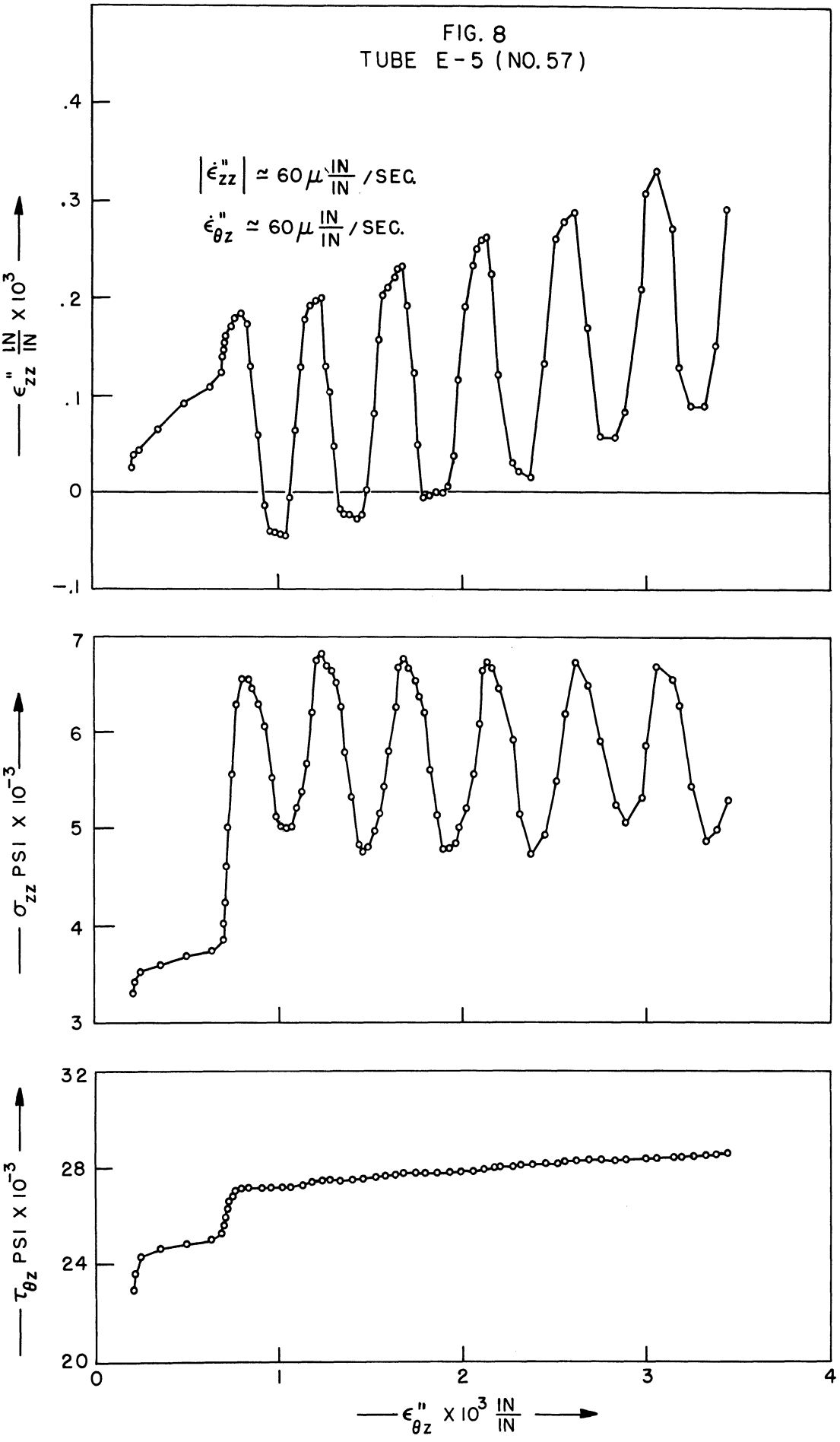
FIG. 8
TUBE E-5 (NO. 57)
$|\dot{\epsilon}''_{zz}| \simeq 60\mu \frac{IN}{IN}$ /SEC.
$\dot{\epsilon}''_{\theta z} \simeq 60\mu \frac{IN}{IN}$ /SEC.
$\epsilon''_{zz} \frac{IN}{IN} \times 10^3$
.4
.3
.2
.1
0
-.1
σ_{zz} PSI $\times 10^{-3}$
7
6
5
4
3
$\tau_{\theta z}$ PSI $\times 10^{-3}$
32
28
24
20
0
1
2
3
4
$\epsilon''_{\theta z} \times 10^3 \frac{IN}{IN}$

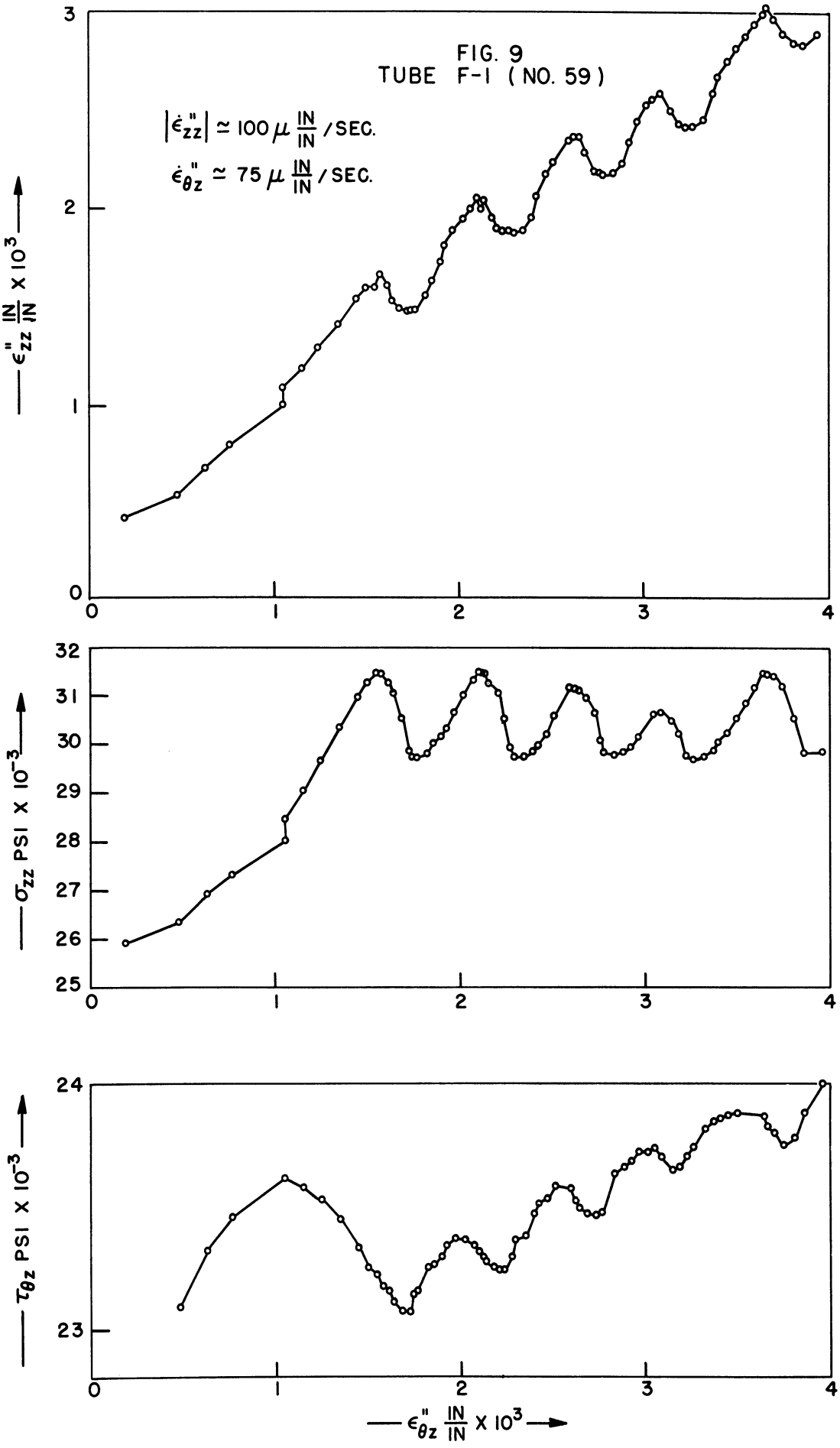
FIG. 9
TUBE F-1 (NO. 59)
$|\dot{\epsilon}''_{zz}| \simeq 100\mu \frac{IN}{IN}$ / SEC.
$\dot{\epsilon}''_{\theta z} \simeq 75\mu \frac{IN}{IN}$ / SEC.
$\epsilon''_{zz} \frac{IN}{IN} \times 10^3$
σ_{zz} PSI $\times 10^{-3}$
$\tau_{\theta z}$ PSI $\times 10^{-3}$
$\epsilon''_{\theta z} \frac{IN}{IN} \times 10^3$

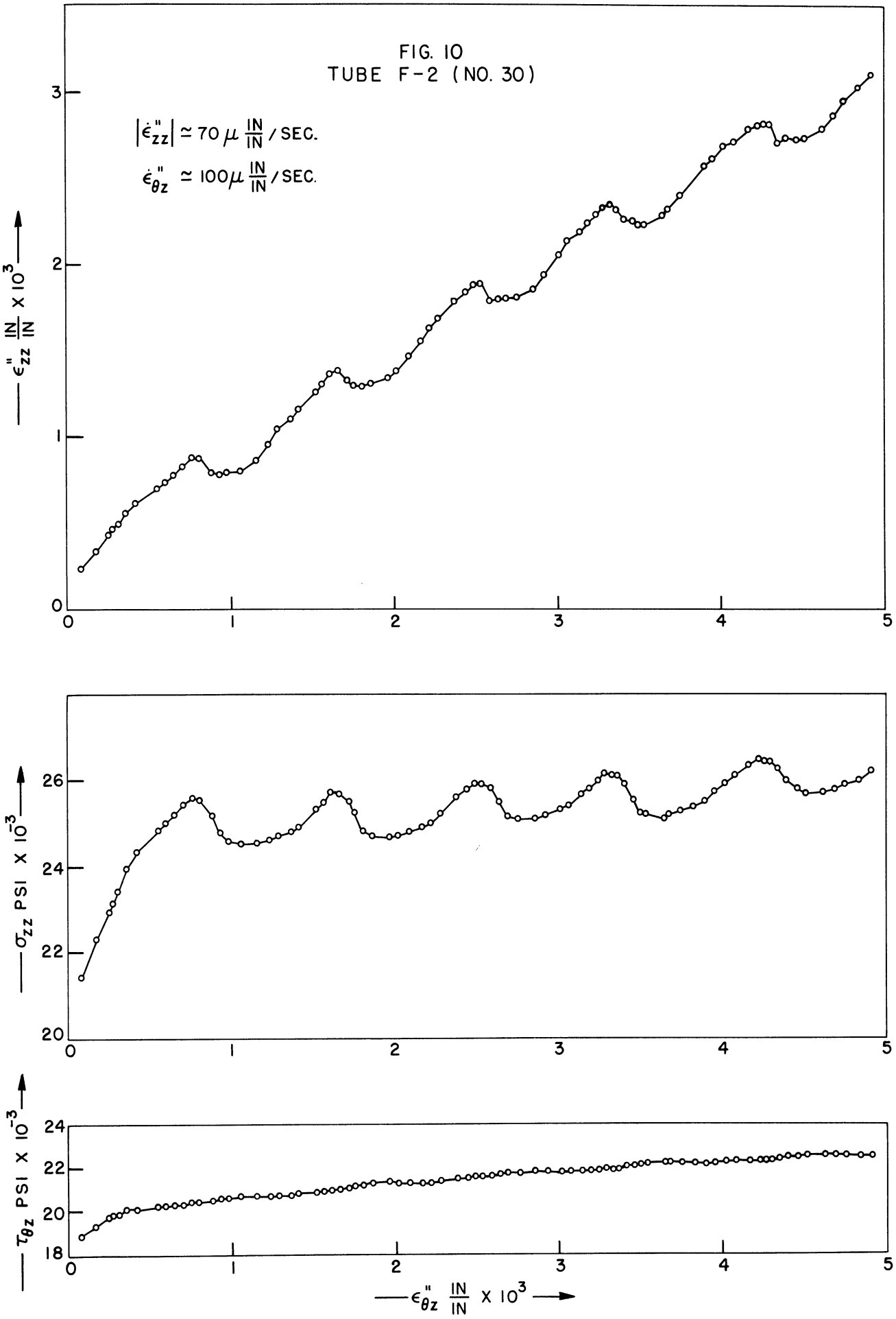
FIG. 10
TUBE F-2 (NO. 30)
$|\dot{\epsilon}''_{zz}| \simeq 70\mu \frac{IN}{IN}$ / SEC.
$\dot{\epsilon}''_{\theta z} \simeq 100\mu \frac{IN}{IN}$ / SEC.
$\epsilon''_{zz} \frac{IN}{IN} \times 10^3$
σ_{zz} PSI $\times 10^{-3}$
$\tau_{\theta z}$ PSI $\times 10^{-3}$
$\epsilon''_{\theta z} \frac{IN}{IN} \times 10^3$

FIG. II
TUBE F-3 (NO. 33)

$|\dot{\epsilon}''_{zz}| \simeq 70\,\mu\,\frac{IN}{IN}$ / SEC.

$\dot{\epsilon}''_{\theta z} \simeq 100\,\mu\,\frac{IN}{IN}$ / SEC.

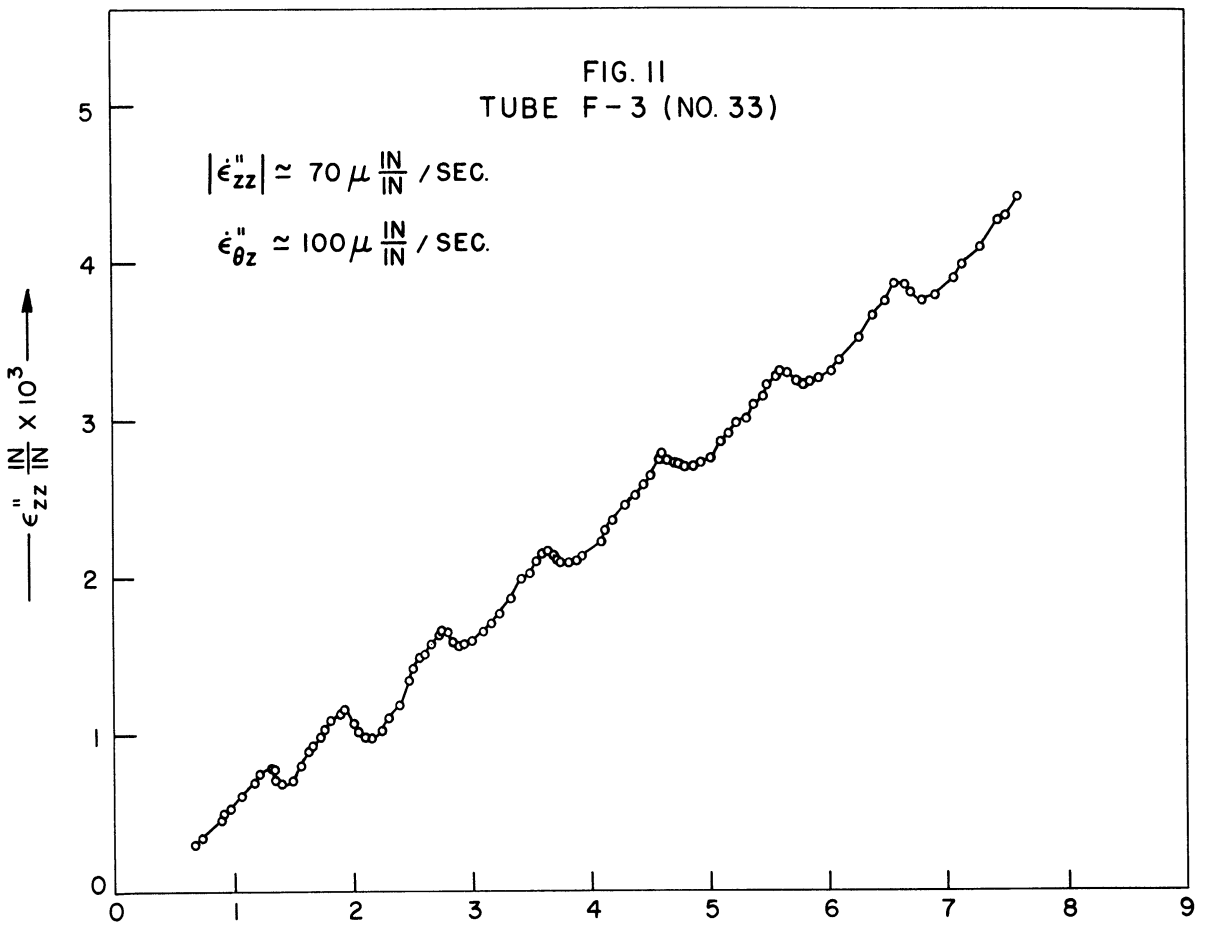

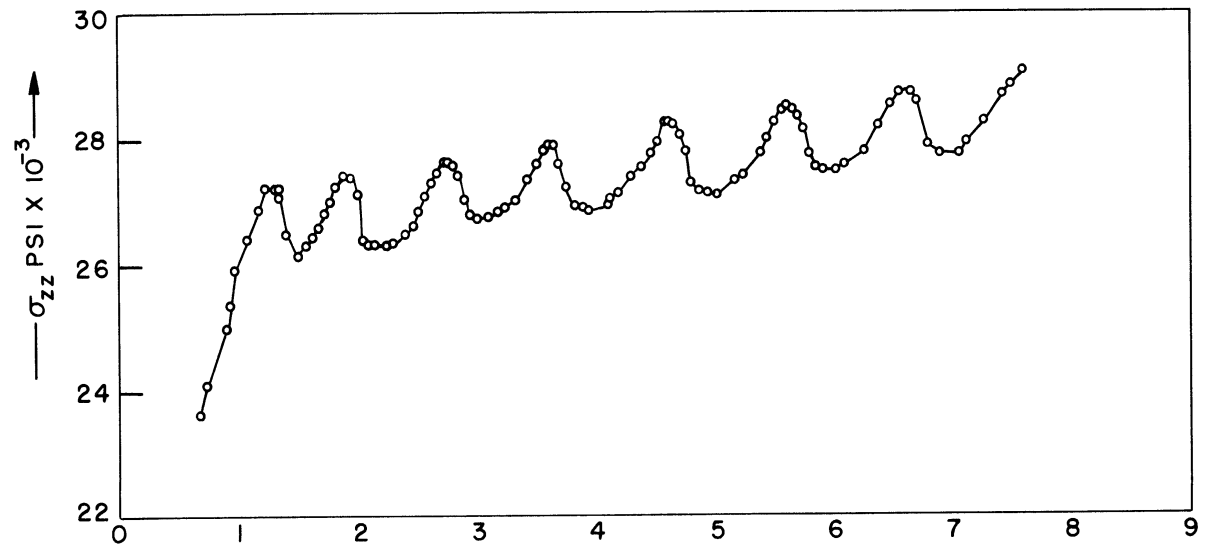

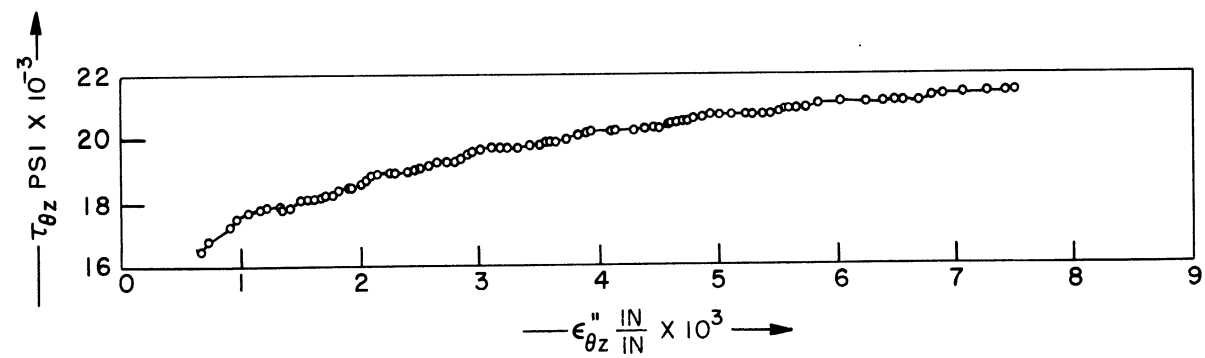

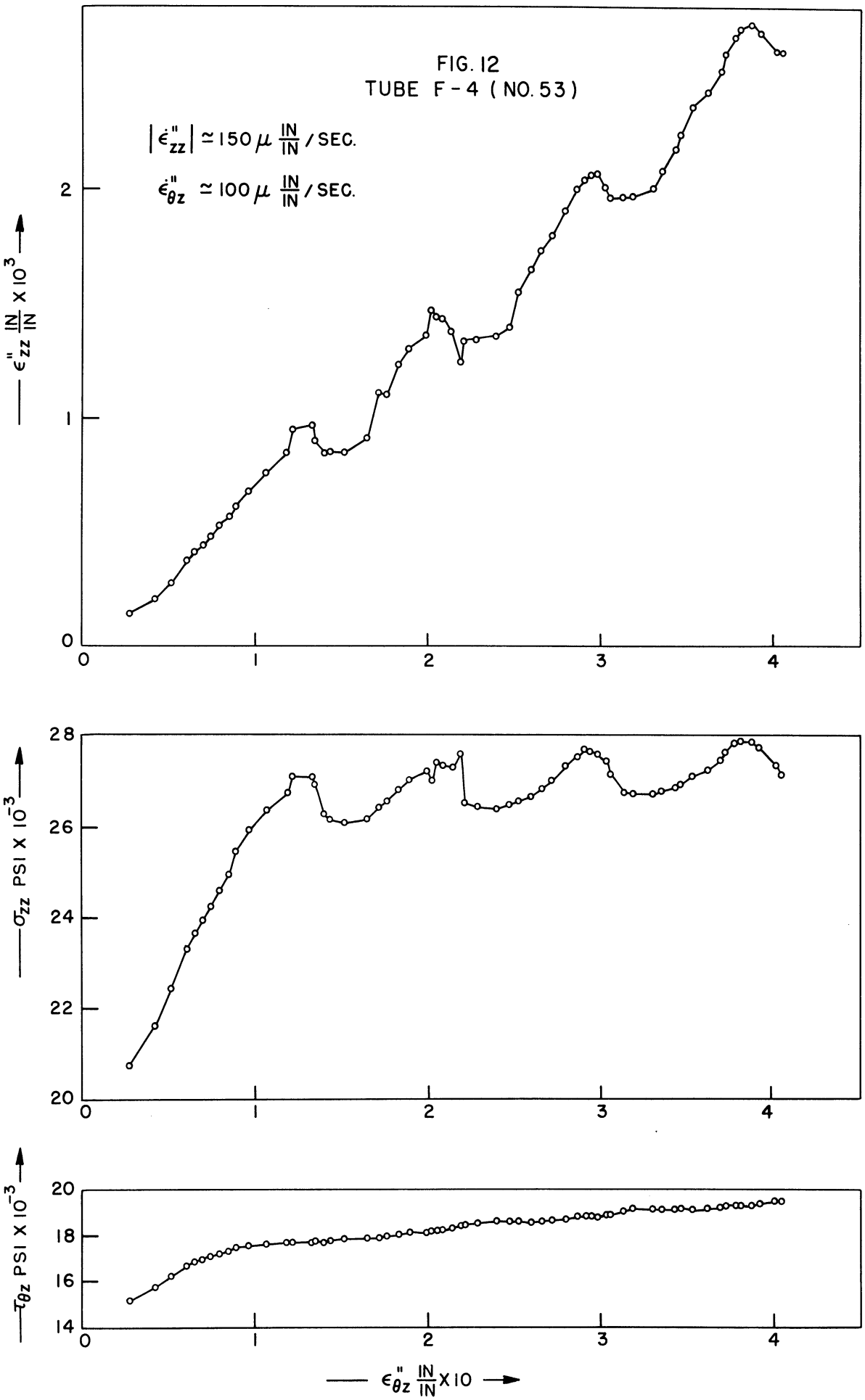
FIG. 12
TUBE F-4 (NO. 53)
$|\dot{\epsilon}''_{zz}| \simeq 150\,\mu\,\frac{IN}{IN}$ / SEC.
$\dot{\epsilon}''_{\theta z} \simeq 100\,\mu\,\frac{IN}{IN}$ / SEC.
$\epsilon''_{zz}\,\frac{IN}{IN} \times 10^{3}$
σ_{zz} PSI $\times 10^{-3}$
$\tau_{\theta z}$ PSI $\times 10^{-3}$
$\epsilon''_{\theta z}\,\frac{IN}{IN} \times 10$

FIG. 13
TUBE F-5 (NO. 54)

$|\dot{\epsilon}''_{zz}| \simeq 50\mu \frac{IN}{IN}$ / SEC.

$|\dot{\epsilon}''_{\theta z}| \simeq 80\mu \frac{IN}{IN}$ / SEC.

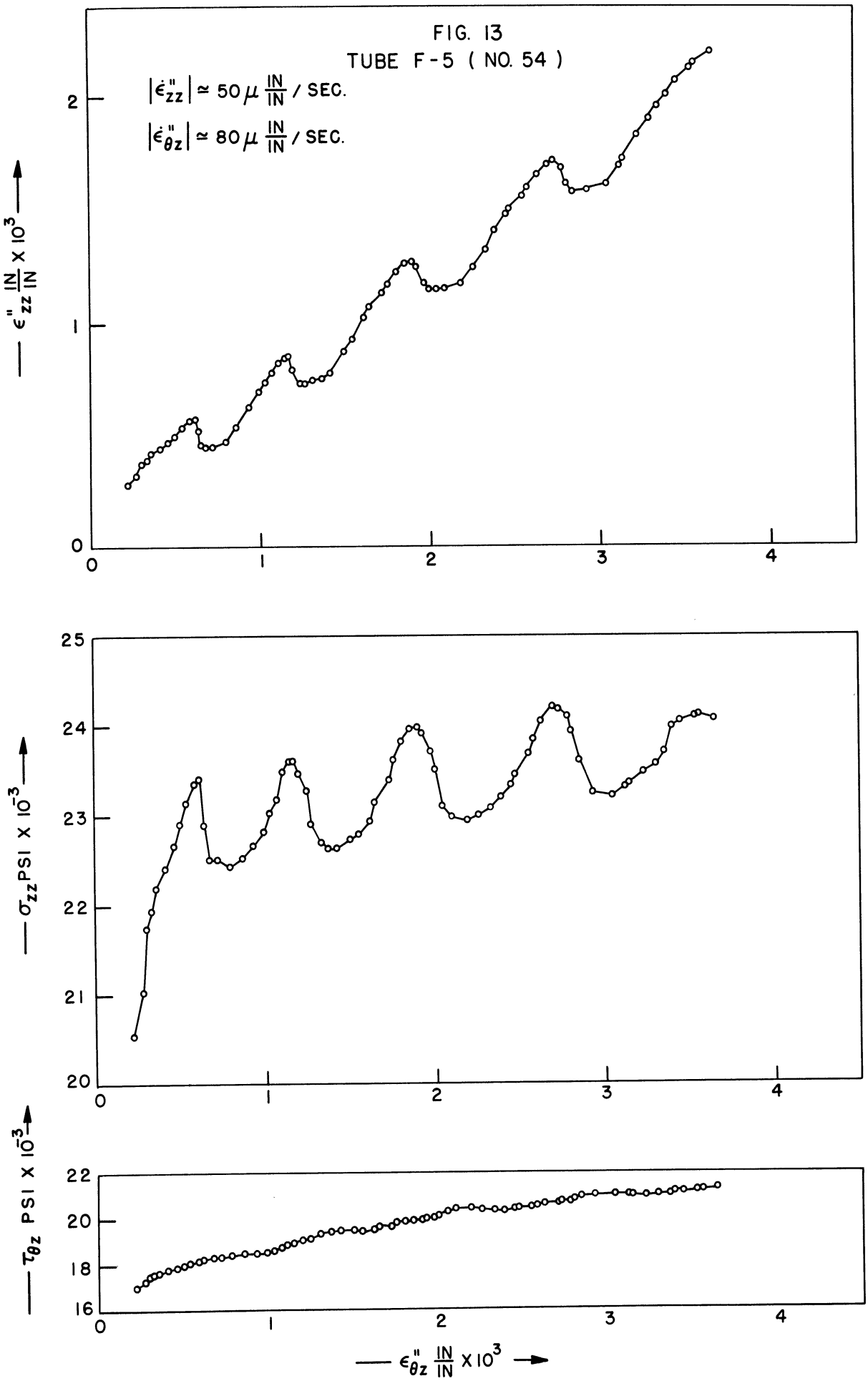

FIG. 14
TUBE G-1 (NO. 30)

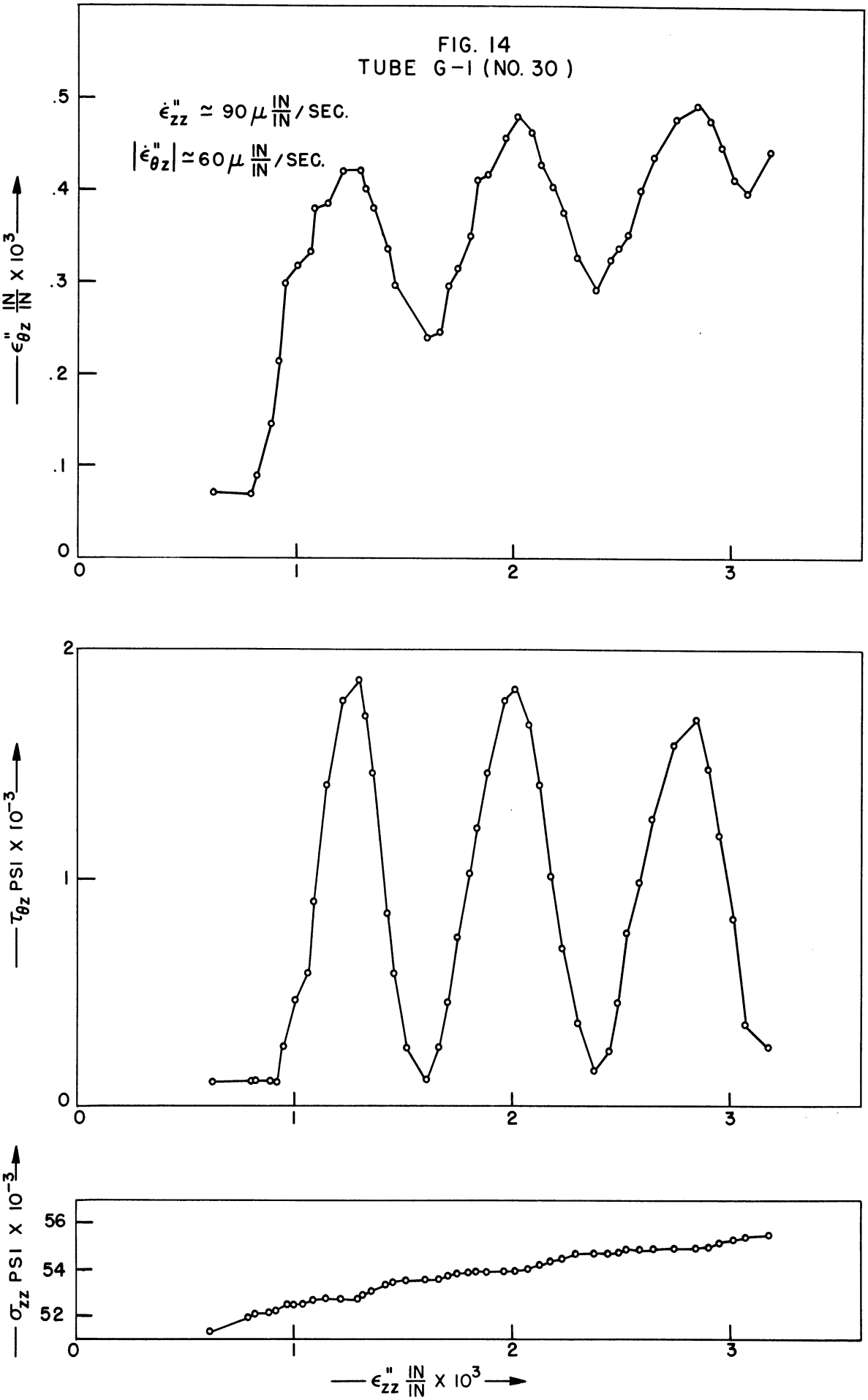

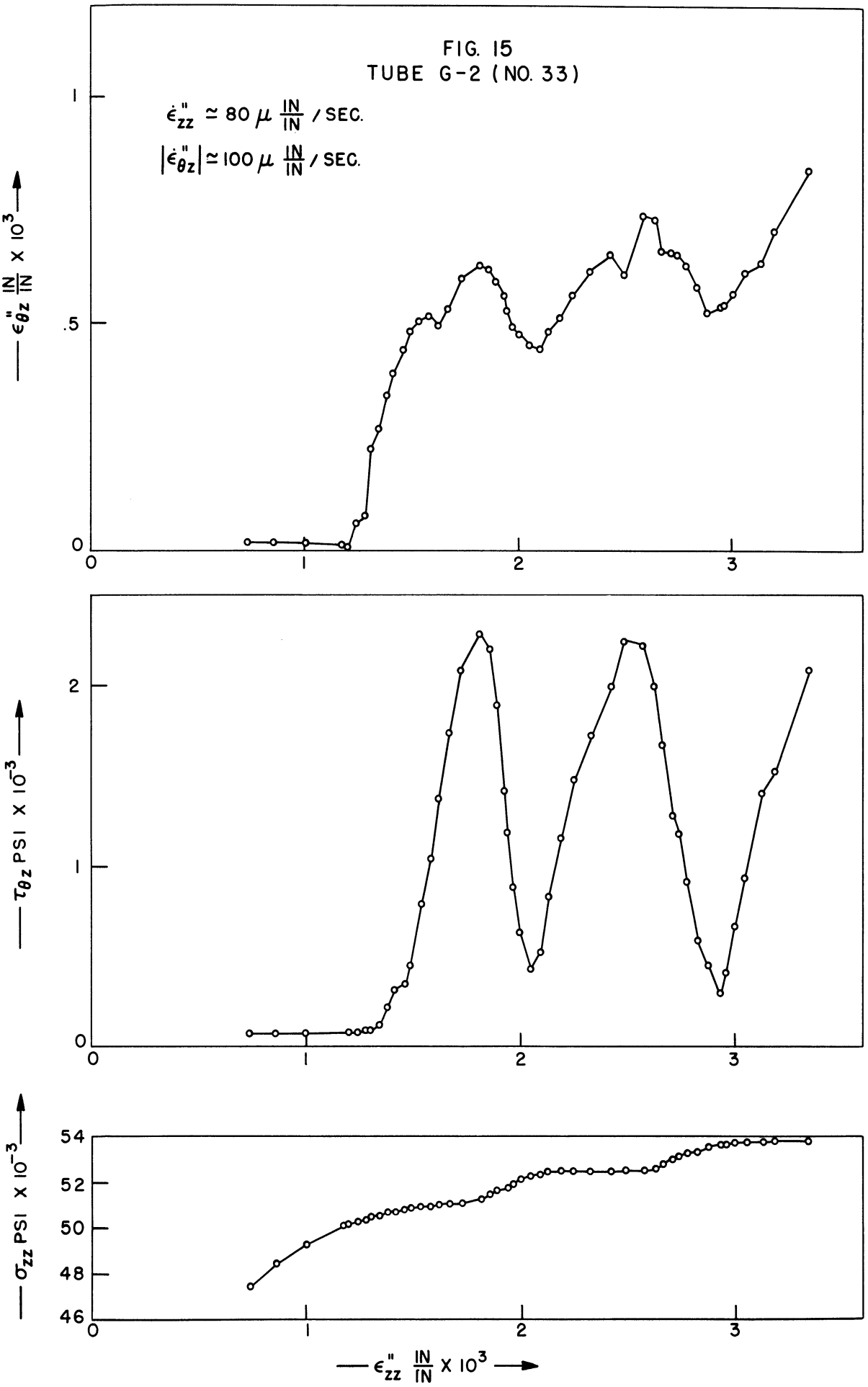
FIG. 15
TUBE G-2 (NO. 33)
$\dot{\epsilon}''_{zz} \simeq 80\,\mu\,\frac{IN}{IN}$ / SEC.
$|\dot{\epsilon}''_{\theta z}| \simeq 100\,\mu\,\frac{IN}{IN}$ / SEC.
$\epsilon''_{\theta z}\,\frac{IN}{IN} \times 10^3$
$\tau_{\theta z}$ PSI $\times 10^{-3}$
σ_{zz} PSI $\times 10^{-3}$
$\epsilon''_{zz}\,\frac{IN}{IN} \times 10^3$

FIG. 16
TUBE G-3 (NO. 53)

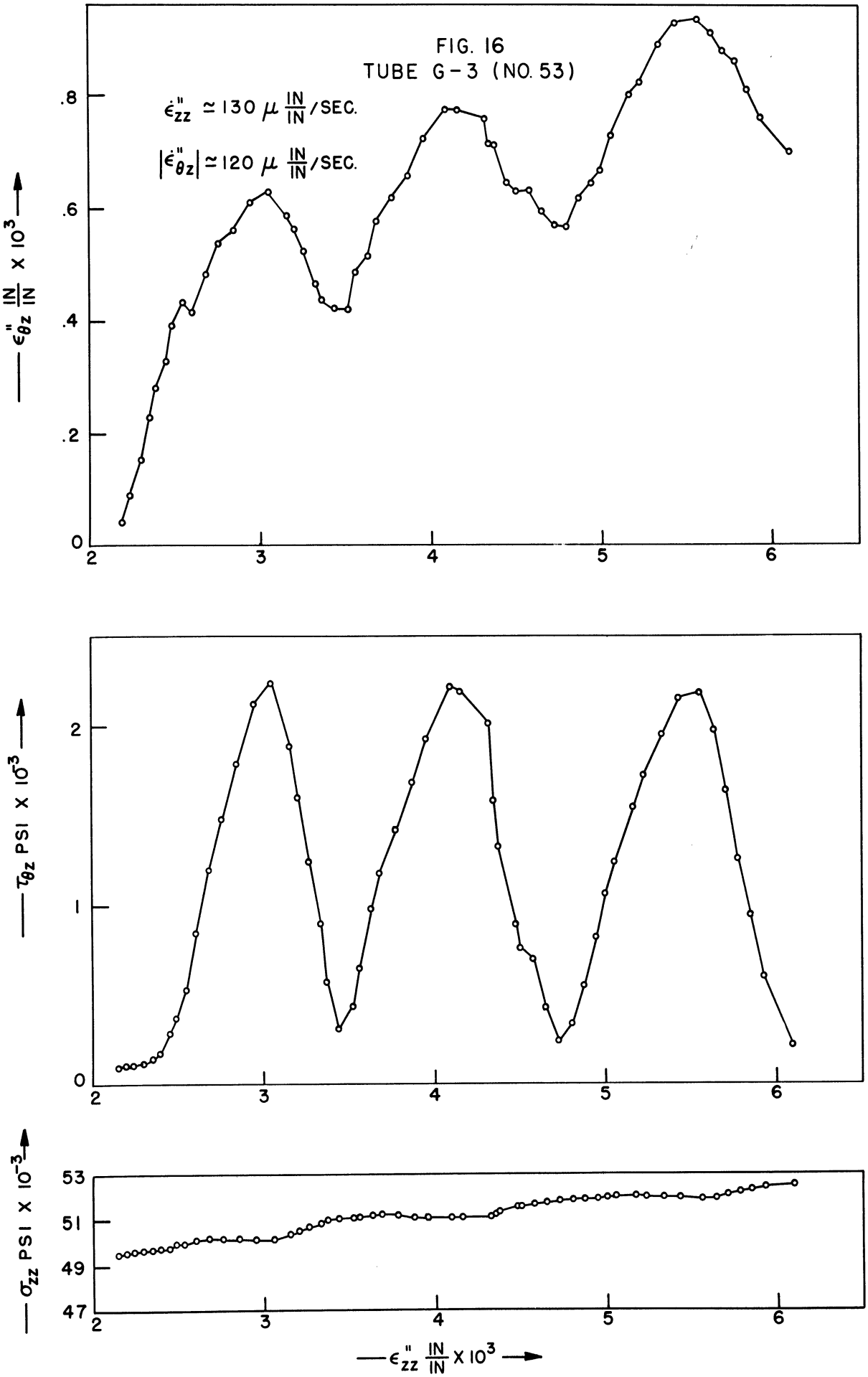

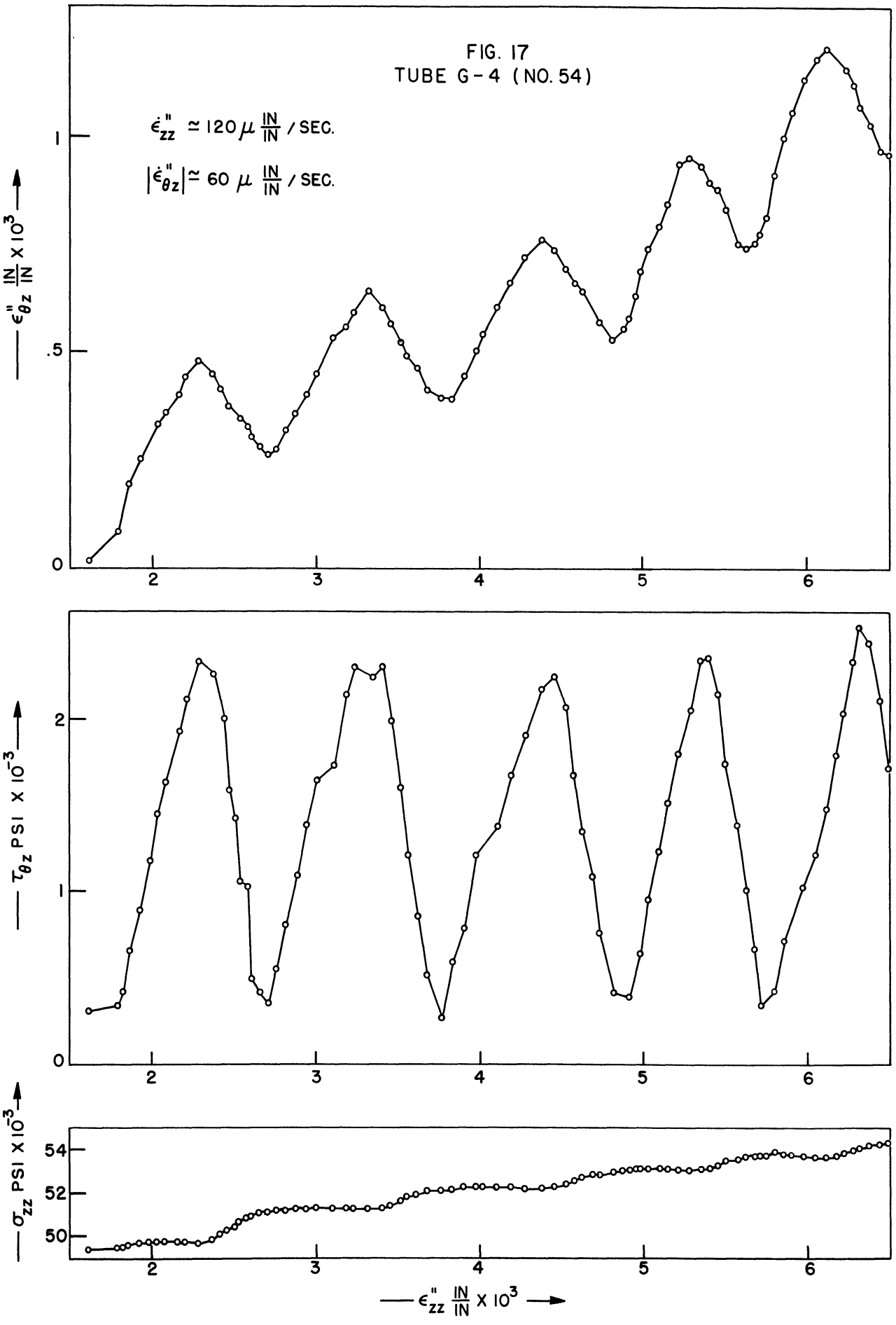
FIG. 17
TUBE G-4 (NO. 54)
$\dot{\epsilon}''_{zz} \simeq 120\mu \frac{IN}{IN}$ / SEC.
$|\dot{\epsilon}''_{\theta z}| \simeq 60\ \mu \frac{IN}{IN}$ / SEC.
$\epsilon''_{\theta z} \frac{IN}{IN} \times 10^3$
$\tau_{\theta z}$ PSI $\times 10^{-3}$
σ_{zz} PSI $\times 10^{-3}$
$\epsilon''_{zz} \frac{IN}{IN} \times 10^3$

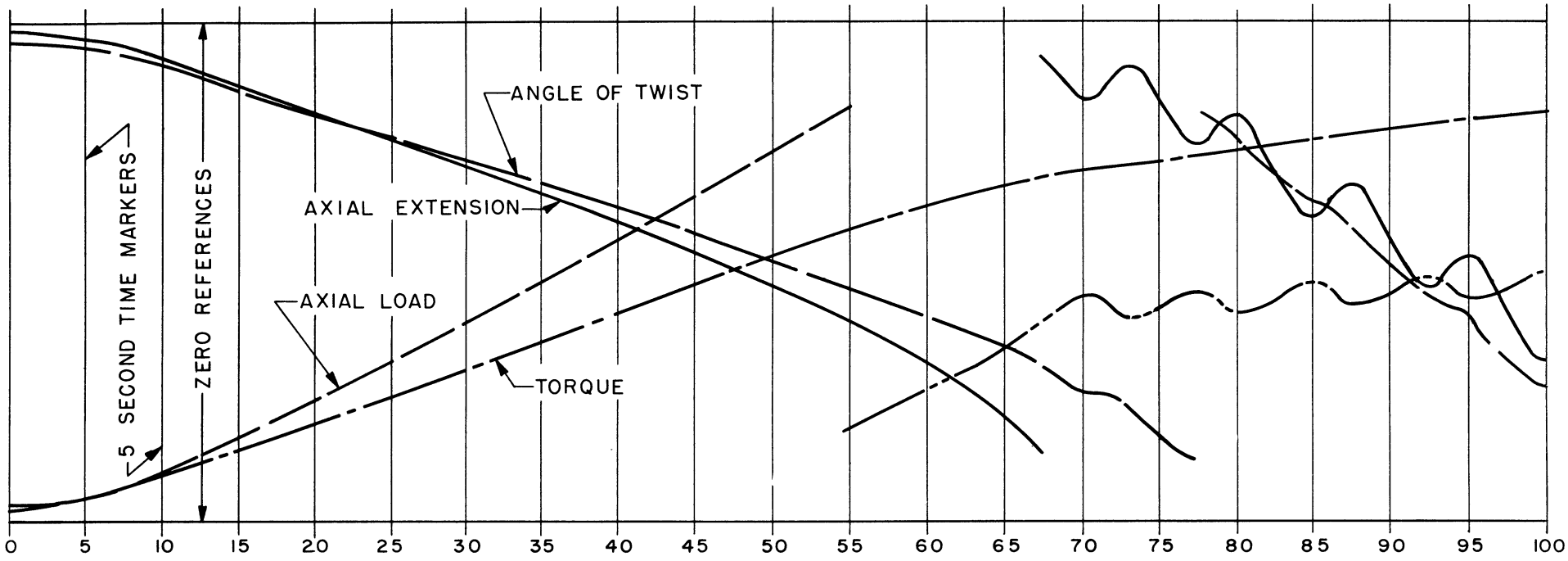

VARIABLE LOADING TEST

THIN WALLED TUBE, SPECIMEN F-3(#54)

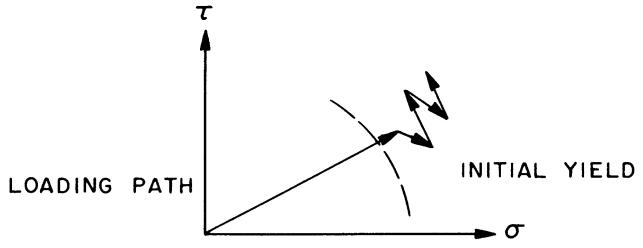

FIG. 18

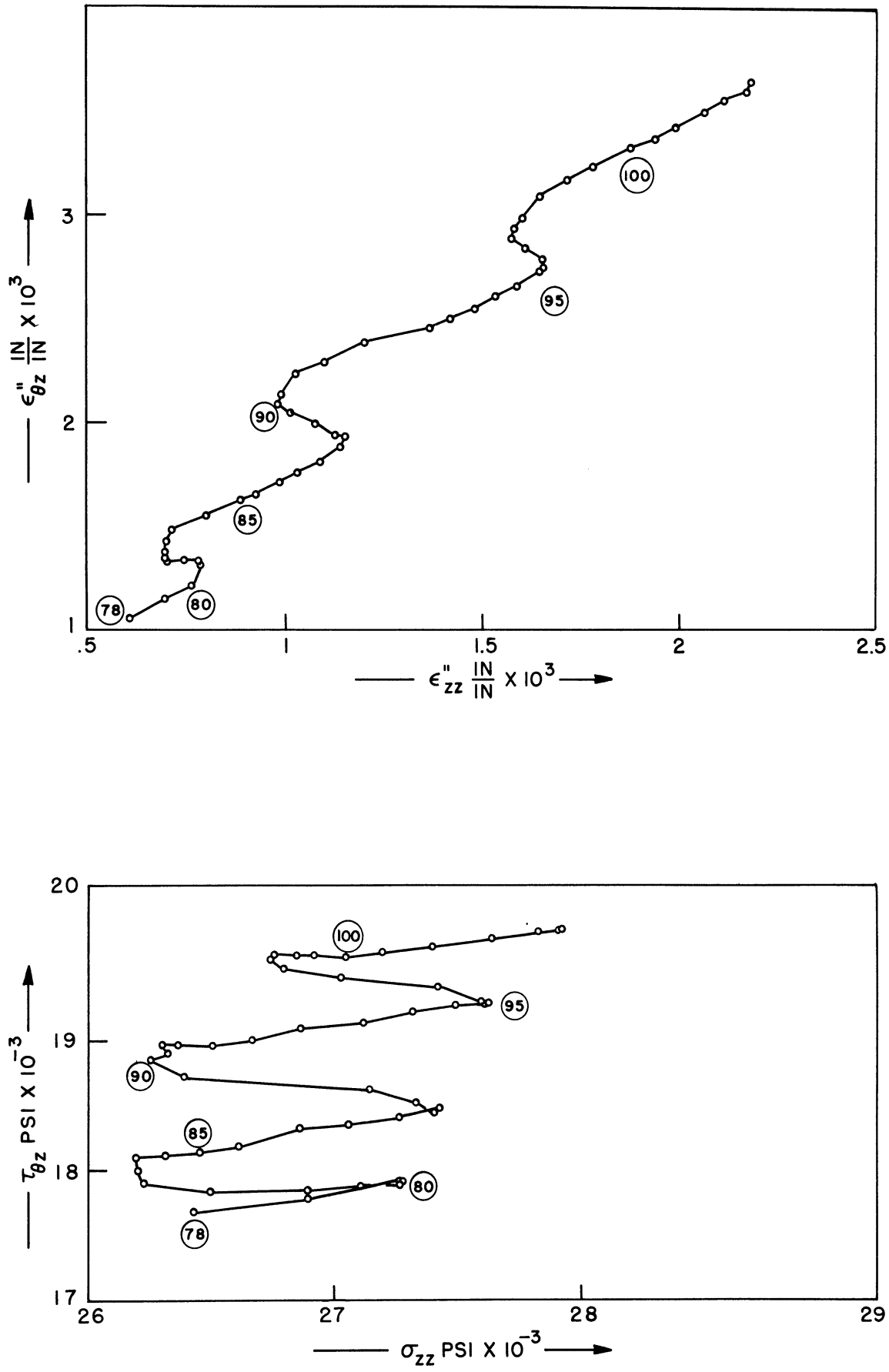

FIG. 19

A portion of the stress and plastic strain paths for tube F-3. Time in seconds is indicated to relate the two curves.